POLITECNICO DI TORINO
Repository ISTITUZIONALE

Analysis of Fan Blade Vibration with a Non-Contact Method

(Article begins on next page)

03 May 2024

Pierluigi PORCO[1], Radosław PRZYSOWA[2], Daniele BOTTO[1]
[1] Politecnico di Torino (Politechnika Turyńska)
[2]Air Force Institute of Technology (Instytut Techniczny Wojsk Lotniczych)

ANALYSIS OF FAN BLADE VIBRATION WITH A NON-CONTACT METHOD

Analiza drgań łopatek wentylatora metodą bezdotykową

Abstract: *Composite fan blades are more and more common both in aviation and ground applications. This work aims to characterize the vibration parameters of plastic blades installed in a wind tunnel fan by a non-contact method, namely blade tip timing (BTT). Blade dynamics was predicted with finite element modelling (FEM) and confirmed experimentally by tip timing measurements and analysis of data. BTT results were acquired and compared in two different configurations. A good agreement between predicted and measured frequency values was obtained for the fundamental mode. Significant differences were observed for the second and third modes due to material anisotropy and contact effects which could not be modelled because necessary material data were unavailable.*

Keywords: blade vibration, composite blade, non-contact measurement, wind tunnel, axial fan, tip timing, vibration analysis

1. Introduction

Fan blades belong to the most stressed parts in turbomachinery [1], because they are simultaneously subjected to different loads such as centrifugal force, vibrations, icing, high speed impacts of foreign objects, erosion and corrosion. Each of them contributes to the acceleration of the blade degradation process, thus attention has to be paid to these factors during the design phase, and their effects must be monitored during the operation of the system.

Since the first gas turbines were designed, one of the most common causes of failure in blades, is combined fatigue due to vibrations: HCF takes place during normal operation and is characterized by high frequencies, while LCF takes places during abrupt variations of speed, which for civil applications is usually limited to ground-air-ground cycles and so is characterized by much lower frequencies.

The number defined by the ratio between vibration frequency and rotational speed of the rotor is called Engine Order (EO) and is fundamental for vibration analysis. For this reason, blade vibration can be classified as follows:

- Synchronous or integral vibration: their frequency is an integer multiple of the rotational speed of the rotor,
- Asynchronous vibration: their frequency is not linked to the rotational speed of the assembly.

One of the main sources of synchronous vibration is the periodic fluctuation of the pressure field seen by the rotating blade during a revolution, caused by stator vanes disturbing the airflow upstream of a bladed assembly. Similarly, asynchronous vibrations are caused by aerodynamic instability phenomena such as flutter and rotating stall. Usually, asynchronous vibration occurs at off-design conditions, while synchronous vibration prevail at particular speed ranges.

The blade vibration parameters are analysed with different approaches depending on whether we are in the design phase or in operation. In fact, during the design phase, one of the main objectives is to verify that the blades do not undergo too large displacements or instability within the speed range of operation, while in operation, the focus lies on monitoring vibration parameters such as amplitude or the natural frequency of blades, because the shifts of these quantities are likely related to the propagation of a crack in a blade [9, 24, 25].

In order to predict and extend the life of blades, it is necessary to know their stress distribution and load frequency during operation. It is not possible to obtain directly the full stress field with the actual measuring systems, so it is necessary to derive it from the measurement of point quantities such as the strain in some spots on the blade's surface or its tip displacement. The latter is delivered by Blade Tip Timing (BTT) which is a non-intrusive and cost-efficient method for blade vibration analysis [21, 26, 27]. FEM modelling complements vibration measurement because it allows the extrapolation of the blade deformation and stress from the tip displacement. From this point of view, the BTT is an indirect method.

Several structural problems and health management approaches were reported for large fan blades installed in ground systems such as wind tunnels [10], cooling fans [6, 13, 14] or desulphurisation systems [19]. Applied methods included strain gauges, laser vibrometry, fast camera image processing [3], shaft torsional vibration analysis [11] and BTT.

Recently, fundamentally new fan designs have been introduced such geared turbofan, UltraFan, propfan or counter rotating fan [12, 23], aimed to increase bypass ratio of gas-turbine engines and reduce CO_2 emissions. What is more, fan blades are often made of non-metallic materials such as fiber-reinforced composites [28, 29] and are operated at much lower rotational speeds than traditional fans and compressors. To reduce risk brought by innovative fan designs, extra care during structural analysis and component certification as well as modern and efficient tools such as BTT are necessary.

This paper investigates the dynamic behaviour of a composite fan blades, which was a part of the wind tunnel. Firstly, FEM model of the bladed disk as well as a Campbell diagram were developed. Secondly, blade tip deflection was observed with a single tip timing sensor. Finally, synchronous resonances were measured by six-sensor BTT system and analysed with Least Squares Fitting.

The vibration results were evaluated and compared with numerical predictions. The proposed methodology and BTT system is well suited for low speed rotating machines and non-metallic blade material.

2. Materials and methods

2.1. Device under test

The system consists of a wooden frame, on which are mounted four fans that a few years ago were used to generate the air flow necessary for the wind tunnel. The fans with 4 composite blades are set in motion by four synchronous three-phase electric engines, which can provide a maximum rotational speed of 1600 rpm each. In nominal conditions, when installed on the wind tunnel outlet, the rotational speed is 1400 rpm, with a flow of 9380 m^3/h and power consumption of 0.55 kW for each rotor. The original power inverter was not available, and so it was used another model of the inverter which worked as well, even though generated some noise in the signals of interest.

The tests were performed on only one of the four rotors. For both the configurations that are described in the following, the tests consisted of acceleration (fig. 1) and deceleration of the assembly, with a rate of about 3.6 rpm/s. The speed range was 400-1600 rpm. In this way, it was possible to identify the occurrence of synchronous vibration even with one single probe.
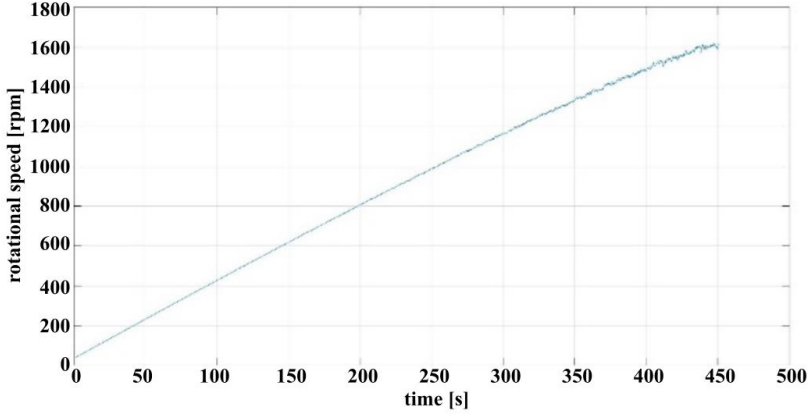
Fig. 1. Rotational speed versus test duration

2.2. BTT system

A standard BTT approach was followed, in which time-of-arrival (TOA) is measured by NI-PXI data acquisition system for every blade pass towards the reference provided by once per revolution signal (OPR). The PXIe-6358 module was used to sample the analogue sensor signal. A Matlab script was developed for determining TOA from waveforms.

The tip displacement D_i in revolution i can be computed multiplying the tip radius r by the time difference between the TOA and a constant reference produced by a notch on the rotor. These values were obtained assuming that the average speed ω remains constant during a complete revolution.

$$D_i = \omega_i r \left(TOA_{blade,i} - TOA_{notch,i} \right) \tag{1}$$

This displacement includes constant component related to the blade equilibrium position which has to be subtracted. The average positions of all blades are called the stack pattern and calculated over the whole test:

$$\theta_0 = \frac{1}{N} \sum_{i=1}^{k} \omega_i \left(TOA_{blade,i} - TOA_{notch,i} \right) \tag{2}$$

where N is the number of complete revolutions during the test and $i = 1 \div N$.

Once the stack pattern is known, the tip deflection d_{ij} of the blade number j can be computed for each revolution:

$$d_{ij} = r \cdot \left(\omega_i \left(TOA_{blade,i} - TOA_{notch,i} \right) - \theta_{0,j} \right) \tag{3}$$

where $j = 1 \div$ number of blades.

344

To process TOA data from several sensors, Least Squares fitting is used, which is described in detail in [7, 8, 17, 18]. Its main assumption is that the tip displacement of each blade is modelled as a sine wave for every revolution. In this way, it can be expressed as follows:

$$d_n = \text{x} \cdot \sin(EO \cdot \theta_n) + \text{y} \cdot \cos(EO \cdot \theta_n) + z \tag{4}$$

where d_n is tip deflection measured by probe n, θ_n is the fixed angular position of the probe n, EO is the known engine order, x and y are estimated vibration parameters and z is a static component. Vibration amplitude A equals:

$$A = \sqrt{x^2 + y^2} \tag{5}$$

2.3. First configuration

The whole assembly (panel + rotors) was set for this first test in a small room that was available for the installation of sensors and for the execution of the tests in different days. The position of the panel was therefore much different than its design purposes. In fact, in this case, the airflow streaming through the panel holes does not have a principal axial direction at the inlet, but the air comes through the bladed disk with a more random distribution of velocity. For this reason, as the speed increases, the rotor has trouble in maintaining the value imposed by the power inverter (fig. 1).

In this configuration, an eddy current sensor pointing towards the notched disk for the One-Per-Revolution (OPR) signal and a single optical sensor for the detection of the blades were used. The probe tip consists of one optical fiber in the middle as transmitter and six optical fibers around as receiver. The employment of a single fiber as a transmitter implies that the signal slope is high, because it takes a very short time for the blade tip to block all the emitted light.

Figure 2 shows a part of the output signal generated by those probes. The dashed lines indicate the threshold levels of voltage at which the trigger was set in order to record the TOA of blades and OPR signals needed for the analysis. The sinus EO1 component in the OPR signal of the eddy current sensor was produced by the rotor misalignment.
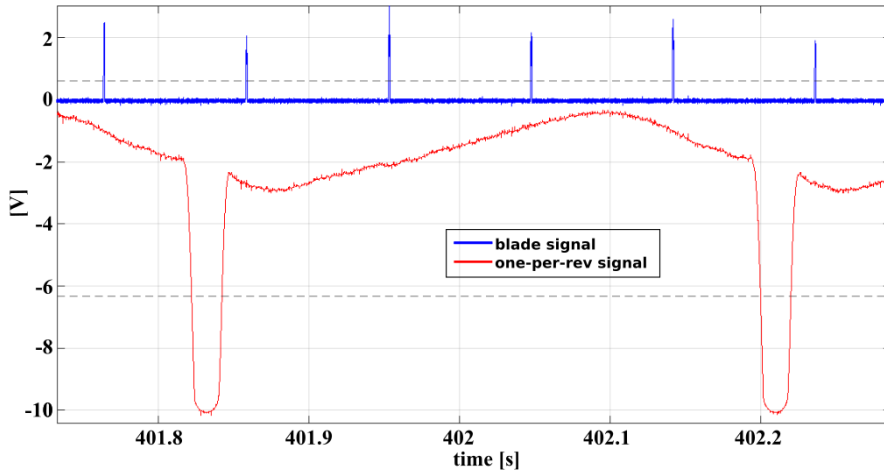
Fig. 2. Signals of the optical BTT sensor and the eddy-current OPR sensor

The employed inverter, as well as irregularities on the surface of the blade, introduced a noise in the signals that had to be taken into account in the MatLab code in order to minimize mistiming errors involving the TOA record that could heavily affect the analysis. For this purpose, it was decided to employ a linear regression fitting of a few points of the signals in the region close to the threshold level.

To measure TOA, a certain number of points before and after the threshold were chosen to be extracted from the signal. The amount of points has been chosen considering the maximum speed of the rotor, because in this case, there are less values nearby the threshold. Knowing the time values and the corresponding voltage levels, it was possible for each signal edge to find a line for each blade passage, computing the slope and the intercept by means of fast matrix operations.

Once the line equation was known, it was possible to compute the TOAs by finding the intersections between the lines and the threshold. Figure 3 depicts a portion of the signal coming from a blade passage, showing the advantages of a linear regression. The black mark corresponds to the point used for TOA after the linear regression has been performed. The red mark is the point before the linear regression. In fact, we can see that all the new TOAs correspond to a signal value equal to the threshold and that the position of each point is approximately in the middle of all the threshold crossings due to noise.
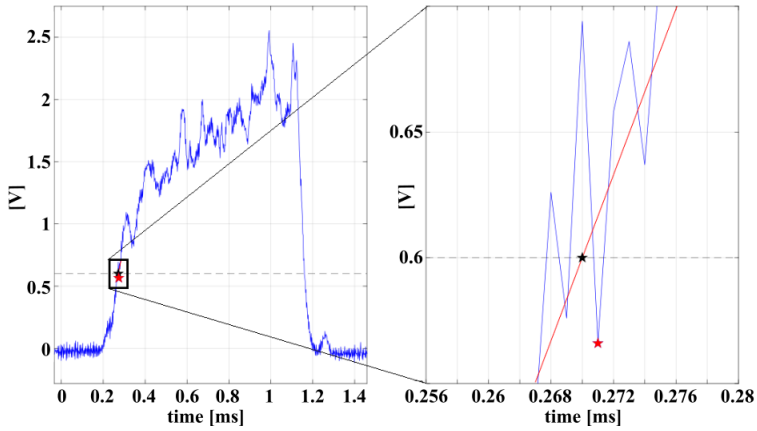
Fig. 3. TOA measurement by linear regression

2.4. Second configuration

The blades that are studied in this work are made of plastic, and therefore it is not possible to use inductive sensors to detect their tip displacements; however it was possible to use a magnetic paint, which was available after the measurement with optical sensors was completed. A few layers of this paint on the blade tips made them detectable by inductive sensors. 6 probes were used for this purpose.

For the OPR signal, a new bracket was designed to fix the optical sensor (used previously to detect blades) to the motor, in the same way as it was done for the eddy current probe. This configuration is depicted in fig. 4.
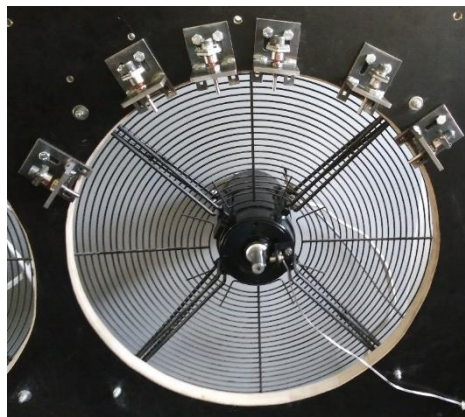

Fig. 4. Picture of the second configuration of probes

347

The positions of probes around the casing/frame are crucial to analyse BTT data. The idea was to exploit a sine fitting algorithm [17] to extract the frequency and amplitude data, so it was possible to choose a non-uniform spacing between the probes. This choice was made, because, in case of a uniform spacing, the system is 'blind' to some engine orders. In fact, if for example, there is an equal spacing of 45°, the system will be blind to all the engine orders which are multiple of 360/45.

Pickering in his master thesis [15] lays the attention on the effect that the probe spacing has on the results. In fact, the condition number of the matrix D0 (see appendix A) should be as close to 1 as possible in order to get the best least square approximation.

For this test, it was possible to mount the frame in its original position at the inlet of a wind tunnel, in this way, it was also possible to see the effects of an obstacle on the blade vibrations.

2.5. FEM model

The structural design process aims to obtain the stress map of the blades produced by the forces acting during the operation of the engine. To reach this goal, it is necessary to develop a finite element model that satisfies the requirements and then validate it experimentally. It is an iterative process, because if calculations do not agree with measurements it is necessary to update the model.

For the geometry acquisition, it was employed a computed tomography system available in ITWL (model GE Phoenix: v/tome/x m 300), while for the mesh and modal analysis, the ANSYS software was used. The principal outputs were the natural frequencies of the blades and the Campbell diagram.

After some analysis of convergence on the first five natural frequencies of a single blade and considering the upper limit on the number of nodes allowed by the license, it was decided to use a combination of brick and tetrahedral elements, with an average size of 9 mm and second order shape functions. In this way, the whole assembly consisting of four blades and the rotor plates was built with 29079 nodes and 10829 elements. In fig. 5, it is possible to notice that the brick elements were employed for the aerofoil, while tetrahedral elements were needed for the complex shape of blade root and rotor plates.
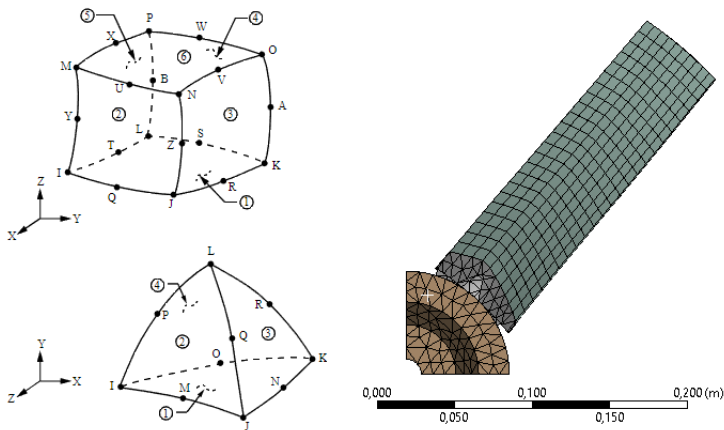
Fig. 5. Mesh detail of a quarter of the assembly

The blade material is a glass-fibre reinforced PPG (polypropylene glycol) manufactured by injection moulding. The material data were available with too low accuracy at first, so it was necessary to identify the correct Young modulus and the damping using experimental techniques such as a hammer test. The coincidence of the first and third natural frequencies was an indicator of the correct elastic modulus, while for the identification of the damping, the Kennedy-Pancu method [4] was employed.

One of the main assumptions made for the model concerns the way in which the blade root is fixed to the rotor. The joint was modelled as a fixed constraint, while in reality the root is clamped between two aluminium disks; thus the real stiffness of the system is lower.

Another issue is related to the material properties because in the model, the blade was considered isotropic, while in reality, this was not exactly true [2]. The reason is that the manufacturing process employed for making the blade is injection moulding. Fibres contained in base material contribute to anisotropy in the stiffness of the component. However, there was not enough material data to model it in a sufficient way.

A proof of this lies in the comparison between the Frequency Response Function (FRF) measured with the hammer test and the FRF computed with the model. It is possible to notice that the second natural frequency, related to a torsional mode shape, differs, while the first and third, related to flexural mode shapes, are coincident (fig. 6).
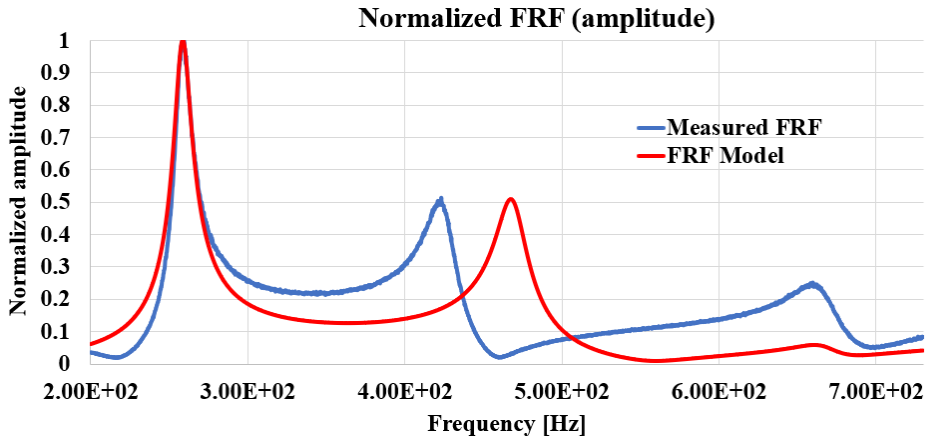
Fig. 6. Results of numerical and experimental modal analysis

3. Results and discussion

3.1. Test 1

This test was aimed to check with a single sensor if any fan blade vibration can be observed. Figure 7 shows a plot of the tip displacements of four blades acquired in the first configuration, with an offset of 0.01 mm between two consecutive blades for clarity.
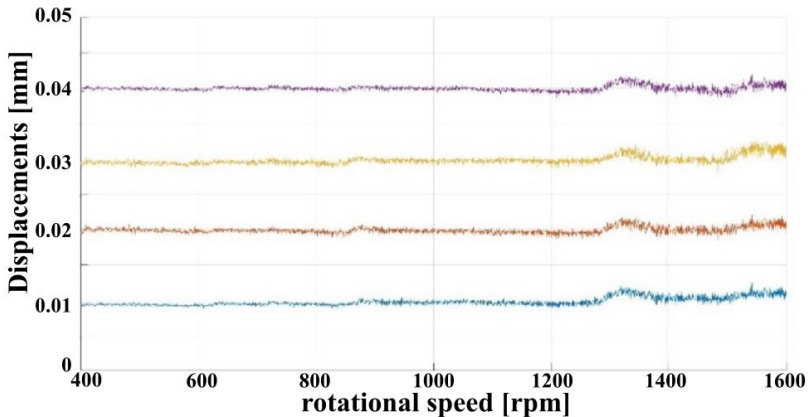

Fig. 7. Tip displacements related to a test performed with increasing speed and optical sensor pointing near the trailing edge

It is necessary to distinguish static and dynamic displacements because they contribute differently to the stress state of the object of study and that is extremely important for the

assessment of fatigue issues. In order to extract the static components, the Savitzky-Golay filter [22] was used, which executes a smoothing of the data by means of a low degree polynomial fitting, performed by the method of linear least squares (fig. 8).
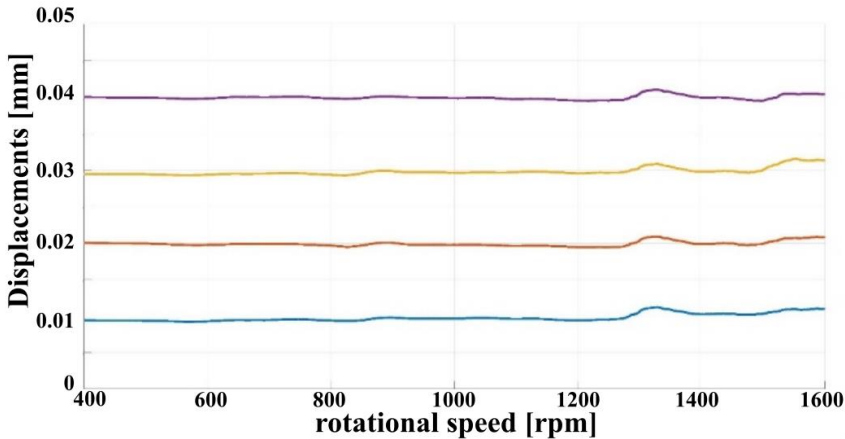

Fig. 8. Low frequency tip displacements

Figure 8 can be used in order to detect any synchronous vibration predicted by the Campbell diagram obtained from the FE model. However, deflection plots should be interpreted with care, especially when a single probe is available. It is not trivial to assert here that the static displacement component changes due to synchronous vibration or not. Moreover, the damping of the material has a substantial impact on the assessment of the displacement plots in relation to numerical predictions because two close resonances can be seen as one and thus, the resulting conclusions will be wrong.

3.2. Test 2

For this test, the frame assembled with the rotor and six sensors was mounted in the wind tunnel, where it was supposed to operate. The test was run twice:
1. Without obstacles (fig. 9a)
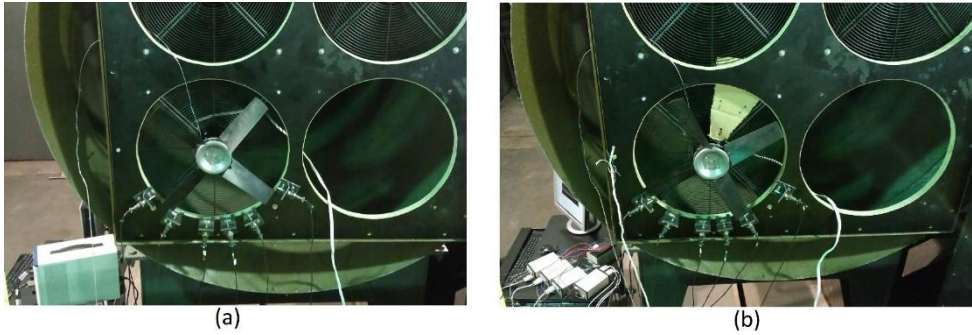2. With one obstacle to excite synchronous vibration (fig. 9b)

Fig. 9. Frame installed on the wind tunnel: a) with free flow and b) with one obstacle

Considering only the tip displacements measured from the timing data of one sensor (fig. 10), it is possible to notice that there is a big difference between the configuration without obstacle and the one with an obstacle on the dynamics of blades. The reason is that the blocker excites not only the first engine order, but also its harmonics, even though its impact is higher for low orders.

When compared to test 1, there is a trend of the equilibrium position of blades in function of speed in fig. 10. This is caused by inductive sensors [26] and unsuccessful zeroing.
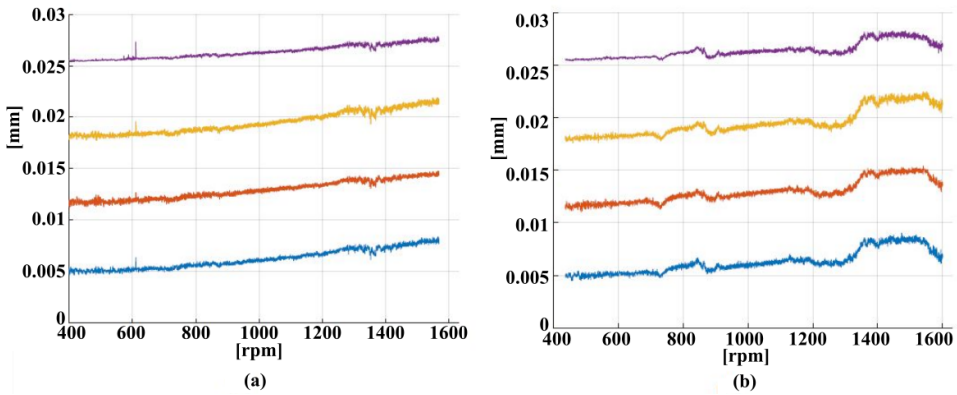

Fig. 10. Tip displacements measured by sensor 5 during acceleration test: a) with free flow and b) with one obstacle

With more sensors it was possible to understand if the static displacements visible in the plots were related to synchronous vibration or not. The reason is that the static displacements of the same blade have different angular positions, as predicted by Heath [5] and shown in fig. 11 concerning the speed range close to 730 rpm.
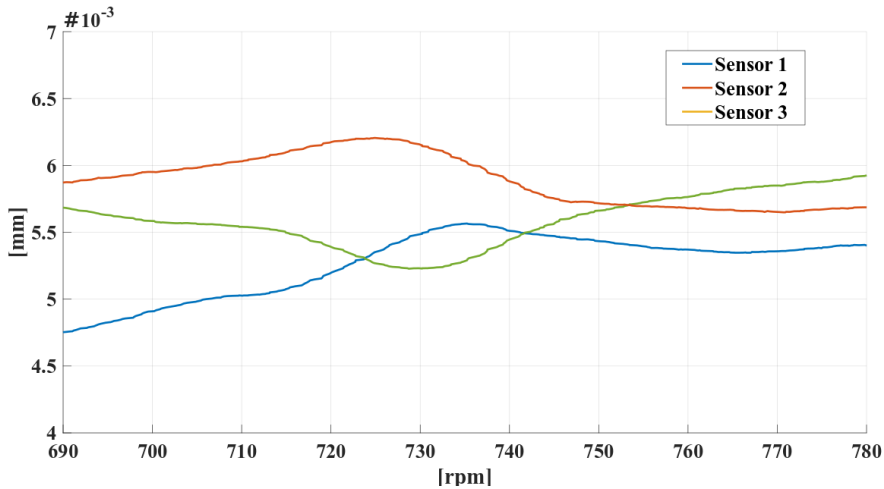
Fig. 11. Quasistatic tip displacements measured by individual sensors

A BTT solver called EMTD Multitool [20] was employed for the Least-Squares analysis of collected data, in order to find the parameters of synchronous resonances. Figure 12 shows the amplitudes of the four blades for the three resonances of mode 1. Their responses are very similar but blade 2 has the highest amplitude.
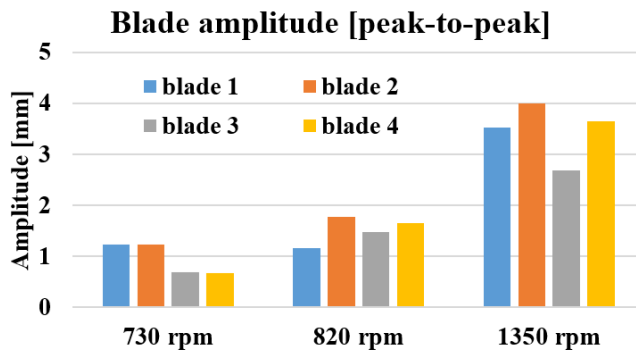

Fig. 12. Amplitudes of the blade tips vibrations corresponding to the detected synchronous vibration

Figure 13 shows a comparison between frequencies predicted by the FEM model (green dots) and estimated by the software (black dots). Coherence (goodness of fit) higher than 90% and low uncertainty were obtained for all three modes and presented resonances. However, it can be seen that a good agreement is obtained only for the vibrations involving the first mode, excited mostly by EO 3, 5 and 6. For these resonances, the model underestimates slightly the vibration frequency. The reason for that lies in the modelling of the joint between the blade root and the rotor. In fact, the real junction is an intermediate

situation between a perfectly fixed root and a free blade, implying that the real resonance occurs at a frequency higher than the perfectly fixed case and lower than the free case.
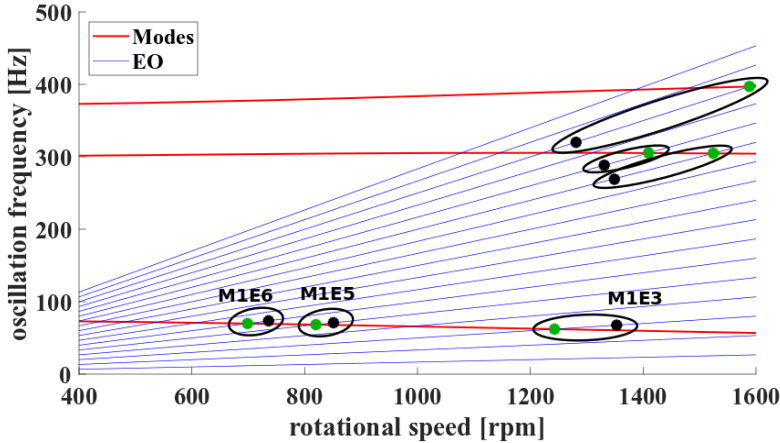

Fig. 13. Campbell diagram with measured and numerically predicted resonances

Regarding the resonances of modes 2 and 3, there is a significant difference between the measurements and the model, so the numerical predictions cannot be considered valid. In this case, an isotropic material assumed in the model turned out not to be the best approximation. However, BTT results for mode 2 and 3 should be accurate because they are characterised by high coherence values.

4. Conclusions

In this work, FEM modelling and BTT method were used to characterize the vibration of a plastic fan blade employed in a wind tunnel. Two different configurations were measured: 1) using only one optical sensor and 2) six inductive sensors for the detection of the blades. The sensor signals were processed using linear regression to measure time of arrival and reduce noise that could lead to unacceptable uncertainty results. In both tests, synchronous resonances responded at similar rotational speeds. In the second configuration, Least Squares were used to estimate the vibration amplitude and frequency.

A finite element model of the blade and the assembly as well as Campbell diagram were made, assuming that material was isotropic. In general, calculations agree with frequency values obtained from the BTT analysis but higher vibration modes were not predicted well. In order to improve this, it is necessary to acquire broader knowledge of the anisotropy of the blade. Further improvements could involve modelling friction at blade roots as this influences the type of constraint and is an additional source of damping.

The article includes selected results from the thesis [16].

5. References

1. Amoo L.M.: On the design and structural analysis of jet engine fan blade structures. Prog Aerosp Sci. 2013;60:1-11. DOI:10.1016/j.paerosci.2012.08.002.
2. Barbero E.J.: Introduction to Composite Materials Design, Second Edition CRC Press 2010.
3. Eberlinc M, Dular M, Širok B, Lapanja B.: Influence of blade deformation on integral characteristic of axial flow fan. Stroj Vestnik/Journal Mech Eng. 54(3), 2008.
4. Ewins D.J.: Modal testing: Theory, practice and application. Research studies press Ltd., second ed., 2000.
5. Heath S., Imregun M.: An improved single-parameter tip-timing method for turbomachinery blade vibration measurements using optical laser probes, International Journal of Mechanical Sciences, Vol. 38, No. 10, 1996.
6. Heinemann T, Becker S.: Axial fan blade vibration assessment under inlet cross-flow conditions using laser scanning vibrometry. Appl Sci. 7(8), 2017, DOI: 10.3390/app7080862.
7. IEEE Standard for Digitizing Waveform Recorders, IEEE Std 1057TM-2007. IEEE 2007.
8. Kaźmierczak K., Przysowa R.: Standard sine fitting algorithms applied to blade tip timing data. Journal of Konbin, Vol. 30, No. 2, 2014, DOI: 10.2478/jok-2014-0012.
9. Kharyton V.: Faults Detection in Blades of an Aviation Engine in Operation, PhD thesis, Ecole Centrale de Lyon, 2009.
10. Kmak F.: Modernization and activation of the NASA Ames 11- by 11-Foot Transonic Wind Tunnel. In: 21st Aerodynamic Measurement Technology and Ground Testing Conference. Vol 53. Reston, Virginia: American Institute of Aeronautics and Astronautics; 2000:1689-1699. DOI:10.2514/6.2000-2680.
11. Maynard K., Trethewey M.: Blade and shaft crack detection using torsional vibration measurements Part 3: Field application demonstrations. Noise Vib Worldw. 2001;32(11):16-23. DOI: 10.1260/0957456011499145.

12. Mileshin V.: A Review of New Experimental Technologies for the Development of Advanced Fans with High Bypass Ratio. Int J Turbomachinery, Propuls Power. 2018;3(3):21. DOI: 10.3390/ijtpp3030021.

13. Muiyser J., Els DN, van der Spuy SJ, Zapke A.: Investigation of Large-Scale Cooling System Fan Blade Vibration. In: Proceedings of the ASME Turbo Expo 2014: Turbine Technical Conference and Exposition. Volume 1A: Aircraft Engine; Fans and Blowers. Düsseldorf, Germany. June 16–20, 2014. V01AT10A008. ASME 2014:1-13. DOI: 10.1115/GT2014-25498.

14. Muiyser J.: Investigation of Large-Scale Cooling System Fan vibration. PhD Thesis. Stellenbosch University 2016.

15. Pickering T. M.: Methods for Validation of a Turbomachinery Rotor Blade Tip Timing System Methods, Masters Thesis. Virginia Tech, Blacksburg, Virginia, USA 2014.

16. Pierluigi P.: Characterization of fan blade vibration with a non-contact method. Rel. Daniele Botto. Politecnico di Torino, Master of Science in Mechanical Engineering, 2019, https://webthesis.biblio.polito.it/13365/

17. Przysowa R., Russhard P.: Non-Contact Measurement of Blade Vibration in an Axial Compressor. Sensors. 2020;20(1):68. DOI:10.3390/s20010068.

18. Przysowa R.: The analysis of synchronous blade vibration using linear sine fitting, Journal of Konbin, Vol. 30, No. 2, 2014, DOI: 10.2478/jok-2014-0011.

19. Przysowa R.: Health monitoring of industrial fan blades in desulphurization system. In 6th EVI-GTI International Gas Turbine Instrumentation Conference. Baden 2013.

20. Russhard P.: MultiTool Blade Tip Timing Acquisition, Analysis and Data Simulation Software; EM0102–Analysis Manual; Technical Report; EMTD Ltd.: Nottingham, UK, 2016.

21. Russhard P.: The Rise and Fall of the Rotor Blade Strain Gauge. In: Sinha JK, ed. Vibration Engineering and Technology of Machinery. Vol 23. Mechanisms and Machine Science. Cham: Springer International Publishing; 2015:27-38, DOI: 10.1007/978-3-319-09918-7.

22. Savitzky A., Golay M.J.E.: Smoothing and Differentiation of Data by Simplified Least Squares Procedures. Analytical Chemistry 1964. 36 (8):1627-39, DOI: 10.1021/ac60214a047.

23. Stepanov A., Fateev V., Mileshin V.: Study of Rotor Blades Vibration Behavior of Counter Rotating Fan Models. In: Volume 7B: Structures and Dynamics. American Society of Mechanical Engineers; 2014:1-10, DOI: 10.1115/GT2014-26310.

24. Szczepanik R.: Early Detection of Fatigue Cracks in Turbine Aero-Engine Rotor Blades During Flight, Journal of KONES. Powertrain and Transport, Vol. 20, No. 1, 2015.

25. Szczepanik R.: Experimental Investigations of Aircraft Engine Rotor Blade Dynamics, Air Force Institute of Technology, Warszawa 2013.

26. Witoś M., Olzak B.: Theoretical foundations of tip timing measurements. In: Bouckaert J.F., Tip timing and tip clearance problem in turbomachines, VKI Lecture

Series 2007-03, von Karman Institute for Fluid Dynamics, Sint-Genesius-Rode, Belgium 2007.

27. Witoś M.: High Sensitive Methods for Health Monitoring of Compressor Blades and Fatigue Detection. Sci World J. 2013;1-31, DOI: 10.1155/2013/218460.

28. Woike M.R., Roeder J.W., Hughes C.E., Bencic T.J.: Testing of a microwave blade tip clearance sensor at the NASA Glenn Research Center. 47th AIAA Aerosp Sci Meet Incl New Horizons Forum Aerosp Expo. 2009:1-14, DOI: 10.2514/6.2009-1452.

29. Wollmann T., Dannemann M., Langkamp A. et al.: Combined experimental-numerical approach for the 3D vibration analysis of rotating composite compressor blades: An introduction. ECCM 2018 - 18th Eur Conf Compos Mater. June 2018.